The Role of Solution Phase Water on the Deposition of Thin Films of Poly(vinylidene fluoride)

Marcel Benz,[†] William B. Euler,*[,†] and Otto J. Gregory[‡]

Department of Chemistry, 51 Lower College Road, University of Rhode Island, Kingston, Rhode Island 02881, and Department of Chemical Engineering, Room 110 Crawford Hall, University of Rhode Island, Kingston, Rhode Island 02881

Received October 5, 2001; Revised Manuscript Received January 8, 2002

ABSTRACT: Thin films of PVDF were deposited from a variety of solution conditions and examined by IR spectroscopy and scanning electron microscopy. Methods to rapidly assess the film thickness and the phase composition of PVDF films have been developed. In particular, the formation of the ferroelectric β phase can be controlled by the composition of the solvent, notably the water content. Using a hydrated salt in the casting solvent reproducibly formed films with high β phase content. However, the water also induces increased surface roughness in the deposited films. The nature of the PVDF films also is influenced by the kinetics of the evaporation process, and this was followed by IR spectroscopy. The rate constants depend on both the film thickness and the gas-phase humidity, indicating that solvent diffusion is an important contributor to both the bulk phase composition and the surface structure of the polymer films.

Introduction

Poly(vinylidene fluoride) (PVDF) is a widely studied polymer due to its ferroelectric, piezoelectric, and pyroelectric properties.[1−5] PVDF occurs in at least four different polymorphs.[6−10] These different crystal structures include the nonpolar α phase and the polar β, γ, and δ phases. In applications where the ferroelectric properties of PVDF are of use it is the oriented β phase that is of most interest. This form can be produced by crystallization under high pressure, poling in a high electrical field, solid-state extrusion, rolling, or stretching of unoriented PVDF films.[11−15] Polymer films are commonly obtained in the α and γ crystalline form when deposited from solution. Few papers describe methods to produce solution cast polymer films in its unoriented β phase.[16−18] PVDF films deposited from HMPA (hexamethylphosphoramide) solutions are reported to have unoriented β-phase crystallinity.[19] However, the toxicity of HMPA limits its use. When DMSO (dimethyl sulfoxide) is used to dissolve PVDF, different polymorphs are found. Some authors found the γ phase to be the crystalline form in DMSO deposited films[20] while others reported the β phase as the resulting polymorph.[21] Thus, there is significant interest in finding a more complete understanding of the controlled preparation of PVDF films when deposited from solution.

In this contribution, we will explain these different results as well as report a simple method to produce unoriented β phase PVDF thin films. We find that when a hydrated ionic salt is codissolved with PVDF and then deposited from solution, films that contain high percentages of unoriented β phase PVDF are formed. The properties of the films are monitored by IR spectroscopy, and by use of standard chemometric techniques we are able to find the IR spectra of pure α, β, and γ phase PVDF. The key to the controlled film growth is the presence or absence of water, which influences both the bulk phase composition and the surface morphology. We also find that there is a strong kinetic influence to PVDF film formation and report our initial studies on the rates of the film formation process of PVDF deposited from solution.

Experimental Section

Polymer Solutions. All solvents and chemicals were used as received from Aldrich and Fischer. PVDF powder was obtained from Aldrich with $M_w \sim 534\,000$. Dimethylformamide (DMF) was added to all the polymer solutions in a concentration of 10% v/v. The PVDF concentration was 50 g/L unless otherwise noted. The polymer was dissolved in a solvent composed of 90% acetone (or other primary solvent) and 10% DMF, sonicated in an ultrasonic water bath below 30 °C for 20 min, and then thermostated at 30 or 37 °C for another 30 min without sonication. All polymer solutions that contained a hydrated salt such as calcium nitrate tetrahydrate were also prepared in acetone/DMF as solvent and 50 g/L PVDF concentration. The concentration range of hydrated salts varied from 0.1 to 40 g/L. Sonication of each solution in an ultrasound water bath followed by heating above 50 °C resulted in complete dissolution of higher concentrations of hydrated salts.

Film Deposition. The polymer thin films were deposited by either casting from solution or spin-coating onto highly polished single-crystal silicon wafers. These wafers were RCA cleaned (rinsed with acetone, methanol, deionized water, and then N_2 dried) prior to use. The complete drying of the polymer film occurred at room temperature or in a temperature-controlled oven at 50 °C. The spin coater from Laurell Technologies Corp. (model WS-400) was programmed for an acceleration rate of 1245 rpm/s, but different maximum angular velocities and spin times were used. To obtain the oriented crystalline form of PVDF, solution-deposited films were stretched at elevated temperatures. The free-standing polymer film is attached in between two clamps of which one clamp is movable in the *x*-direction. The clamps are separated by an attached weight. The polymer film is coupled to a temperature-controllable hot plate movable in the *z*-direction. The stretching temperatures were set between 110 and 150 °C. The temperature control in the polymer film is ±10 °C, which had no effect on the results reported here. A stretching ratio of up to 3 could be achieved with the described setup.

Film Measurement. The thickness of dried polymer films on the silicon wafers was measured with a Sloan Dektak IIA profilometer. Free-standing films could not be measured with a profilometer. Thus, a free-standing film was clamped in

[†] Department of Chemistry.
[‡] Department of Chemical Engineering.
* To whom correspondence should be addressed. e-mail: weuler@chm.uri.edu.

10.1021/ma011744f CCC: $22.00 © 2002 American Chemical Society
Published on Web 02/28/2002

between two aluminum foils of known thickness. This three-film structure was placed into a cylindrical mold and the mold filled with two-part epoxy. After the epoxy had cured, the exposed sandwich structure was polished and evaluated with a reflection light microscope (Nikon, model 104). IR spectroscopy was performed using a Perkin-Elmer model 1650 FTIR spectrometer at 2 cm^{-1} resolution. To follow the evaporation process of a drying polymer film, two techniques were used. To observe this process from beginning to the end, a fixed-angle (~16°) specular reflectance accessory from Perkin-Elmer was used. The second method was to start the IR measurements after the film was removed from the wafer (after 20 min). The film was then placed on the IR sample holder and was firmly attached with tape to avoid any shrinking of the film during the drying process. Only absorbance values in the recommended Beer's range ($0.2 \leq A \leq 0.7$) were used for kinetic analysis. The temperature for all of the kinetic measurements was 23 ± 1 °C. The infrared spectral manipulations such as baseline correction, offset, and integration were performed with the computer program Grams/32 AI (version 6.00) (Galactic Industries). Rate constants were found by nonlinear least-squares fitting using the routines in SigmaPlot v5.0. Scanning electron microscopy was performed using a JEOL JSM-5900LV instrument.

Results and Discussion

Infrared Spectroscopy. Film thicknesses can be measured using profilometry or microscopy, but a faster, more convenient and nondestructive method was required for this work. Thus, the IR absorbance was used to measure the polymer film thickness according to Beer's law, $A = \alpha t$, where α is the absorption coefficient and t is the thickness. The challenge was to find an absorbance band in the IR spectrum of PVDF that was isolated from other bands and, more importantly, with an absorption coefficient reasonably independent of the crystalline phase of the polymer (α, β, or γ).

The α and γ phases of PVDF could be produced by deposition from solution with different temperature and humidity drying conditions. Films with an increased amount of the β phase (but still containing some α or γ phase) were obtained by stretching the polymer at elevated temperature as described in the Experimental Section. Spin coating was chosen as the deposition technique in order to obtain constant thickness across the film. Different thicknesses of the polymer films were obtained by increasing the PVDF concentration from 50 to 75 g/L or by varying the spin-coating speed from 200 to 1500 rpm. By comparing the IR spectrum of the three polymorphs of PVDF, it became clear that only two bands seemed to be independent of the crystalline phase, 1404 and 1070 cm^{-1}. The thickness and the IR absorption of the two IR bands of a large number of PVDF films were measured and evaluated to find a correlation among them. We found that the absorbance band at 1070 cm^{-1} was independent of all three crystalline forms. The second absorbance band at 1404 cm^{-1} was sensitive for the thickness measurement of α and γ phase films but could not be used for films containing the β phase because it did not show a linear correlation. The results are shown in Figure 1. The plot shows a good correlation between the IR absorbance and the film thickness with $A = 0.095t + 0.07$ ($R^2 = 0.97$), where A is the absorbance at 1070 cm^{-1} and t the film thickness in micrometers. The linear equation for the 1404 cm^{-1} IR absorbance was $A = 0.207t + 0.10$ ($R^2 = 0.98$). Thus, the 1070 cm^{-1} IR absorbance was used for all further determinations of film thickness, and the 1404 cm^{-1} IR absorbance was used to verify the thickness for α and γ phase films.

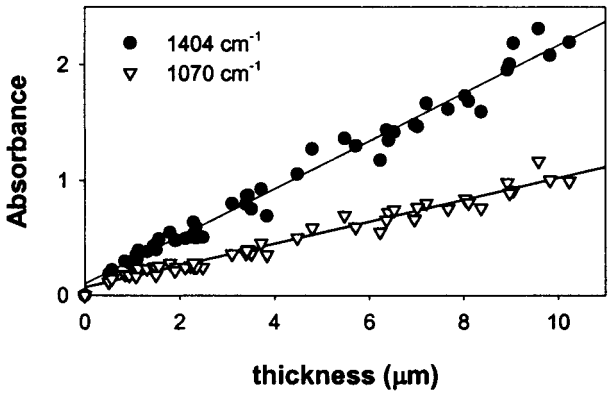

Figure 1. Plot of IR absorbance vs polymer film thickness: circles, absorption band at 1404 cm^{-1}; triangles, absorption at 1070 cm^{-1}. The best fit lines are $A = 0.095t + 0.07$ ($R^2 = 0.97$) for the 1070 cm^{-1} peak and $A = 0.207t + 0.10$ ($R^2 = 0.98$) for the 1404 cm^{-1} peak.

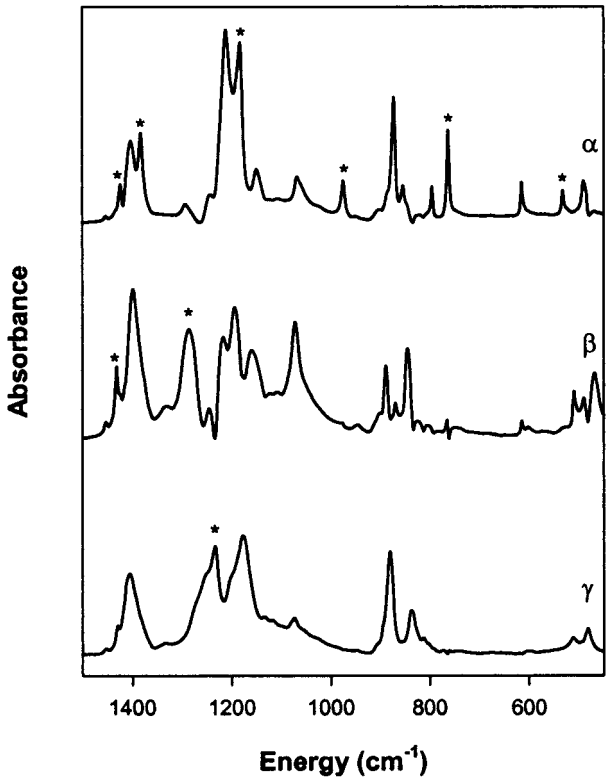

Figure 2. IR spectra of the predicted spectra of pure components of PVDF: top spectrum, α form; middle spectrum, β form; lower spectrum, γ form. The asterisks in the spectra indicate the characteristic IR bands for that phase. The IR spectra were calculated with principal component analysis (PCA).

Although spectral features for each phase have been previously identified,[22−27] the IR spectrum for each of the pure α , β , and γ phases has not been reported. For instance, in the case of α phase PVDF, even when produced from the melt and quenched in liquid nitrogen, the IR spectra always indicated traces of γ crystallinity.[28] By means of a large number of PVDF spectra, which vary in composition of each phase (α, β, and γ), and principal component analysis (PCA), we were able to obtain the IR spectrum of each pure component, as shown in Figure 2. The α crystalline polymorph presents the most easily distinguishable form. It has representative IR bands at 1423, 1383, 1210, 974, 762, and 532 cm^{-1}. The β and γ phases are very similar, and only a

Table 1. Solvents Tested[a]

solvent	dipole moment (D)	phases observed
nitrobenzene	4.22	not soluble
dimethyl sulfoxide (DMSO)	3.96	γ
acetonitrile	3.92	γ
dimethylformamide (DMF)	3.82	γ
dimethylacetamide (DMA)	3.81	γ
acetone	2.88	γ
glycerol	2.6	not soluble
tetrahydrofuran (THF)	1.75	α and γ
benzyl alcohol	1.71	not free-standing
ethanol	1.69	α
isopropyl alcohol	1.56	α
cyclohexanone		α
toluene	0.37	α
xylene (o, m, p)	~0.1	not soluble
1,4-dioxane	0	not free-standing
cyclohexane	0	not soluble

[a] A polymer solution of 50 g/L was prepared at elevated temperature with each solvent (90% solvent and 10% DMF). The cast films were dried at 80 °C at a relative humidity of less than 10%.

few IR bands distinguish each crystalline form. The β phase has two representative IR bands at 1431 and 1286 cm^{-1}, while the γ phase can be distinguished with its characteristic 1234 cm^{-1} IR band. We do not have any concrete information how the amorphous part of PVDF influences the IR spectra since PCA was not able to reliably determine the spectrum of the amorphous phase.

Bulk Phase Composition. As mentioned in the Introduction, there are few solvents reported in the literature that produce the PVDF crystalline β phase when deposited from solution, with different beliefs about whether DMSO is one of them. When we performed the deposition from DMSO, we obtained PVDF films with mixed β and γ phase when the relative humidity exceeded 50% but only the γ phase for humidities below this. To understand this behavior, we deposited the polymer from a variety of solvents, listed in Table 1. It is evident that solvents with a higher dipole moment produce PVDF films with γ phase crystallinity, while solvents with lower dipole moment result in the nonpolar α form.

To further investigate the role of water in the deposition of PVDF, different polymer solutions with water contents of 2−30 g/L were prepared. The water was added to the solvent prior to the polymer dissolution to prevent precipitation of the polymer. While none of the solutions gave any β phase PVDF, the added water did effect the surface morphology of the polymer (vide infra). We speculated that the lack of the β phase was caused by water rapidly evaporating from the polymer/solvent system, thereby preventing the formation of the PVDF β phase. Therefore, a different procedure to add water to the polymer solution was tested. By adding hydrated or hygroscopic salts, we ensured that the water remained in the drying polymer film during the crystalline phase growth. The following salts (to saturation) were added to an acetone/DMF solution of PVDF: calcium chloride (hygroscopic), calcium nitrate (hygroscopic), calcium nitrate tetrahydrate, cobalt perchlorate hexahydrate, strontium chloride hexahydrate, tetrapentylammonium chloride (hygroscopic), toluenesulfonic acid monohydrate, and tris(2,2′-bipyridine)ruthenium(II) chloride hexahydrate. All of the hydrated/hygroscopic salts induced some degree of β phase in the solution deposited films. When other, nonhydrated or nonhygroscopic but soluble salts such as calcium sulfate or sodium tetraphenylborate were added to an acetone/DMF PVDF solution, none of the deposited films had any detectable β phase. In comparison, the use of dehydrated (but hygroscopic) $Ca(NO_3)_2$ vs $Ca(NO_3)_2 \cdot 4H_2O$, the amount of the β phase, indicated by the IR absorption at 1286 cm^{-1}, decreased notably for the anhydrous salt. Owing to the good solubility in acetone/DMF, calcium nitrate tetrahydrate was used for all further experiments involving a hydrated salt.

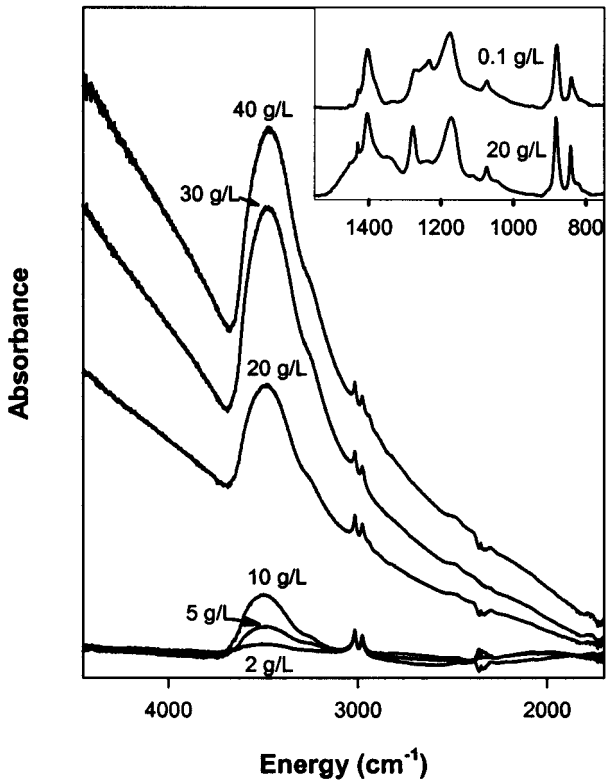

Figure 3. IR spectra of PVDF films formed under different conditions. PVDF solutions (acetone/DMF) with different concentrations of $Ca(NO_3)_2 \cdot 4H_2O$ (2−40 g/L) were spin-coated at 500 rpm for 30 s and subsequently dried at 50 °C are compared. The scattering profile between 1500 and 4000 cm^{-1} reflects the surface morphology roughness, which goes along with the whiteness appearance of the film surface. Transparent films (no baseline slope) are obtained with solutions containing less than 10 g/L hydrated salt. The inset shows the IR fingerprint range of the sample with 0.1 g/L (upper spectrum) and 20 g/L (lower spectrum) $Ca(NO_3)_2 \cdot 4H_2O$. Note the peak near 1286 cm^{-1}, indicative of the β-phase.

Several PVDF solutions with different amounts of calcium nitrate tetrahydrate were prepared (0.1, 0.5, 1, 2, 5, 10, 20, 30, and 40 g/L hydrated salt). The solution deposited and subsequently dried polymer films were compared with IR spectroscopy. The most notable changes, as demonstrated in Figure 3, are the size of the OH stretching peak near 3500 cm^{-1} and the slope of the background. The OH peak increases with increasing amount of the hydrate, as expected. The background slope is associated with surface roughness—those samples with increasing water content become increasingly rough.[29] The β phase marker band near 1286 cm^{-1} appeared in every film and increased in intensity as the concentration of hydrated salt increased. At low salt concentrations, the films are mixtures of β and γ phases as indicated by the marker bands near 1286 and 1234 cm^{-1}, respectively, and contain essentially no α-phase, as indicated by the lack of a peak at 974 cm^{-1}. At high

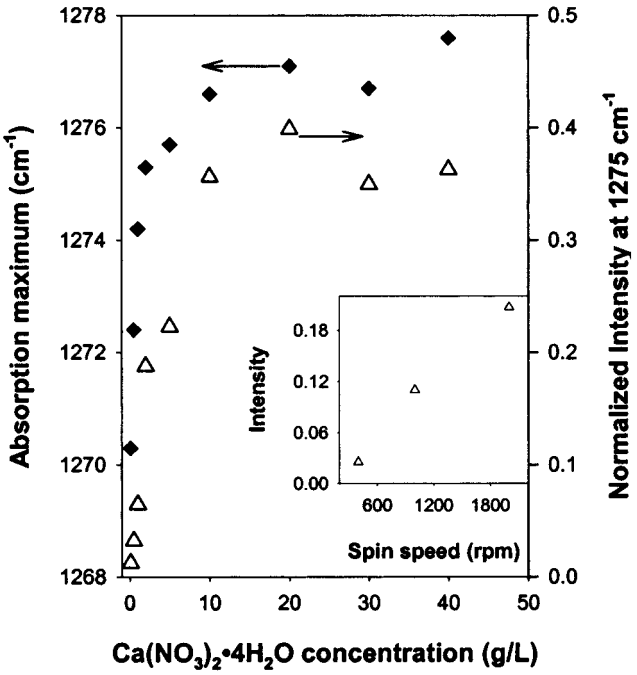

Figure 4. Effect of the addition of $Ca(NO_3)_2 \cdot 4H_2O$ on the phase of PVDF films. PVDF solutions (acetone/DMF) with different concentrations of $Ca(NO_3)_2 \cdot 4H_2O$ (2−40 g/L) were spin-coated at 500 rpm for 30 s and subsequently dried at 50 °C are compared. Diamonds show the wavelength shift of the β phase marker peak indicating IR band toward higher wavelength with increased salt concentration. Triangles show the normalized and baseline corrected absorbance increase of the same band with hydrated salt concentration. The inset shows the effect of rotational velocity on the β-phase marker peak for a solution with 5 g/L $Ca(NO_3)_2 \cdot 4H_2O$.

salt concentrations, the films are only β phase. The IR spectra of two films (0.1 and 20 g/L $Ca(NO_3)_2 \cdot 4H_2O$) are shown in the inset of Figure 3. We also observed that the β phase marker band near 1286 cm^{-1} band shifted toward higher wavenumber with increased salt concentration. The band shifted from 1270 cm^{-1} at the lowest salt concentration to 1279 cm^{-1} at the highest salt concentration, but with little change for concentrations above 20 g/L. The absorbance maximum followed the same profile, as shown in Figure 4. The small feature at about 1400 cm^{-1} arises from nitrate ion remaining in the film, suggesting that the observed shift found in the 1286 cm^{-1} marker band may be caused by a weak interaction of the PVDF with nearby calcium ions. The inset of Figure 4 shows the effect of spinning speed on films created using a PVDF solution with 5 g/L $Ca(NO_3)_2 \cdot 4H_2O$. As the film is spin-coated at higher rotational velocity, an increased amount of β-phase is found. This suggests that the rate of the solvent evaporation, which is controlled by the rotation rate during spin-coating, is a critical factor in determining the bulk phase composition in these films.

Surface Morphology. The same set of samples with different concentration of $Ca(NO_3)_2 \cdot 4H_2O$ also resulted in different surface morphologies. We previously reported the effect of humidity on the surface morphology of solution deposited PVDF.[29] We found that films deposited from a solution prepared at temperatures greater than 50 °C and at relative humidities greater than 40% possessed a rough, opaque surface, but other preparation and deposition conditions resulted in transparent, smooth films. We also correlated the increase in surface roughness with the IR scattering profile in the 1500−4000 cm^{-1} region and thus the degree of the white appearance.

In this work, similar effects were noticed with the increased concentration of the hydrated salt. All samples were spin-coated at low humidity (23%) and subsequently dried at room temperature. Therefore, on the basis of our previous work, their surfaces would be expected to be transparent and smooth and have a flat baseline in the IR spectrum between 1500 and 4000 cm^{-1}. However, only samples with concentrations less than 10 g/L of the calcium salt actually resulted in a transparent film. All of the samples with higher than 10 g/L $Ca(NO_3)_2 \cdot 4H_2O$ gave a white surface morphology, which resembled the PVDF films deposited at higher humidities. The scattering profile of the IR spectra is shown in Figure 3. The baseline slope between 1500 and 4000 cm^{-1} is horizontal in the films with less than 10 g/L hydrated salt (transparent) and increases with increased salt concentration.

Lai et al.[30] previously described the appearance of "cloudy" polystyrene film when deposited with hygroscopic solvents, which was explained as due to the rapid precipitation of the polymer with water. A similar rapid precipitation of PVDF at the surface of drying films exposed to sufficient levels of water appears to account for the rough surface we observe. We examined the surface morphologies of three different opaque/white films with SEM. Figure 5A shows a film that was prepared by using an acetone/DMF solution of PVDF dissolved at ∼50 °C and that was deposited at high humidity conditions (relative humidity = 64%). The polymer film in Figure 5B was prepared by adding calcium nitrate tetrahydrate to a solution prepared at room temperature and deposited at low humidity (23%). Finally, Figure 5C shows a film that was deposited from a solution prepared at low temperature with no salt and by spraying water on the drying film to force a precipitation of the polymer. The SEM micrographs indicate that all three films have a similar surface morphology, although the size of the fibrils in the microstructure does vary. This supports the conclusion that the opaque/white surface appearance is due to precipitation of the polymer with water.

Although pure water added to a PVDF solution did not induce formation of the unoriented β phase, it did have an effect on the surface morphology of the resulting spin-coated polymer thin film. PVDF solutions with different concentrations of water added to the solvent were prepared, ranging from 0 to 30 g/L. The polymers were dissolved at 37 °C, giving good solubility except for the 30 g/L solution, which was turbid. The thickness of the spin-coated films were constant (1.6 ± 0.1 μm from profilometry), except the 30 g/L solution, which deposited a thinner film, 0.4 μm. When deposited via spin coating at low humidity (38%), most of the films were opaque in the center and transparent on the edges. The size of the white center increased with increased water content in the polymer solution. Photographs of these results are shown in Figure 6. Optical micrographs of the polymer films were similar, exhibiting starlike patterns, well-known with spin-coated polymer films.[31,32]

The surface morphology could also be controlled using different spinning speed when spin-coated from an acetone/DMF solution of PVDF dissolved at 37 °C (53% relative humidity, with no H_2O added). At low rotational velocities transparent films were formed, but using the

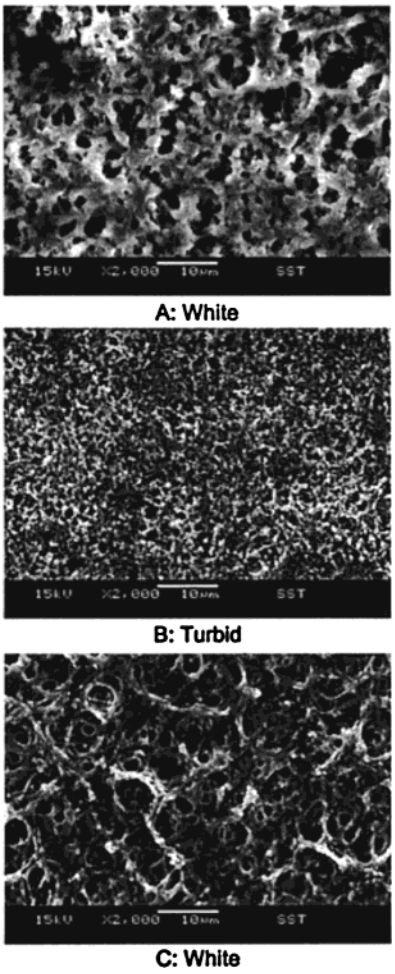

Figure 5. SEM pictures of three polymer films with white surface appearance. A is a film from a PVDF solution dissolved at temperature greater than 50 °C and deposited at a relative humidity greater than 50%. B shows a film from a solution containing 20 g/L hydrated calcium nitrate. C displays the picture of a film whose surface was precipitated by spraying water on the fresh deposited film.

same polymer solution and at the same humidity, high rotational velocities resulted in opaque, white films. Increasing the spin speed changed both the evaporation rate and the film thickness. To differentiate between the two effects, polymer films were deposited at the same spin speed but with different spin times in order to vary only one parameter, the average velocity of the solvent front, which is related to the evaporation rate.[33] Thus, a polymer film with the slowest solvent evaporation rate, 5 s spin time, had a transparent appearance while a spin time of 10 s resulted in an opaque/white center and transparent edge. Finally, a 15 s spin time gave a fully white polymer film. This indicated to us that the surface morphology was a kinetically controlled process since the thickness of the spin-coated film remained the same (2.1 ± 0.1 μm).

Kinetics. To study the influence of the water evaporation rate on the polymer thin film characteristics, the evaporation process of a solution deposited film was observed with IR spectroscopy. The amount of water in a film was followed by integrating the −OH vibrational profile around 3500 cm^{-1}. Although the first overtone of the carbonyl stretch is in the OH stretching region, it was deemed of insignificant area to affect results.

PVDF films were cast onto silicon substrates, and after enough evaporation had occurred to remove the

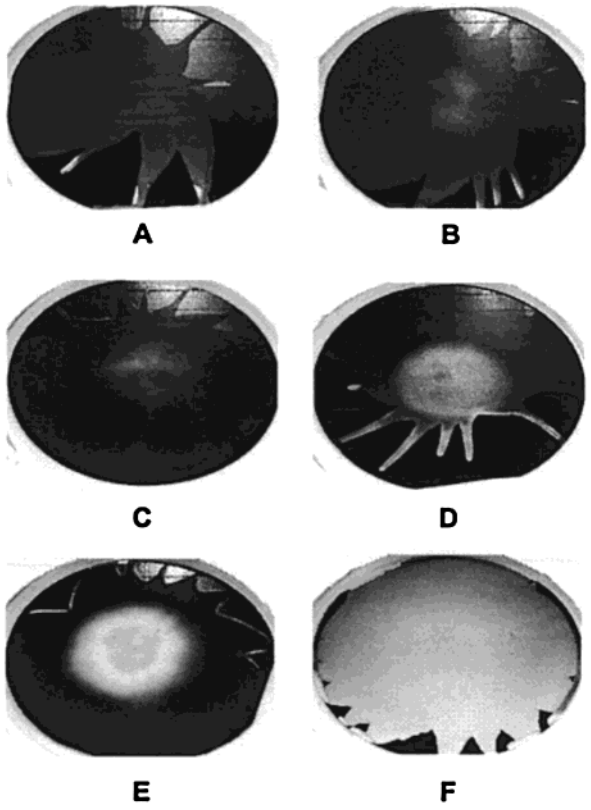

Figure 6. Photographs of spin-coated films prepared with different concentrations of water added to the solvent: A, 0; B, 2 g/L; C, 4 g/L; D, 8 g/L; E, 16 g/L; F, 30 g/L. The polymer films are transparent; the gray color is due to the underlying silicon substrate. Note that the diameter of the white region in the center of the photograph increases from A to F.

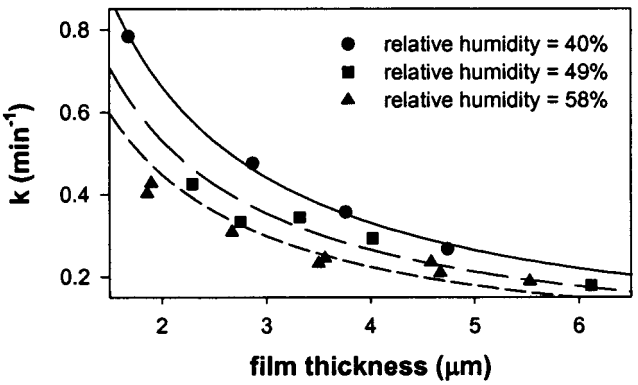

Figure 7. Rate constants found for the loss of water as a function of film thickness at different humidity levels. The first-order rate constants were found by fitting the integrated area of the OH region from the IR spectra taken on free-standing films starting approximately 20 min after the films were cast. The lines are fits to the function k = constant/t.

films (~20 min), these free-standing films were followed by IR spectroscopy for the remainder of the film formation process. The integrated area for the removal of water followed first-order kinetics in all cases. The first-order rate constants varied with film thickness and the gas phase humidity, as demonstrated in Figure 7. The rate constants, k, can be fit modestly well to the function k = constant/t, where t is the film thickness, shown as the lines in Figure 7.

A few experiments were done where IR spectra of the cast film on the silicon wafer were followed using specular reflectance IR spectroscopy, thereby eliminat-

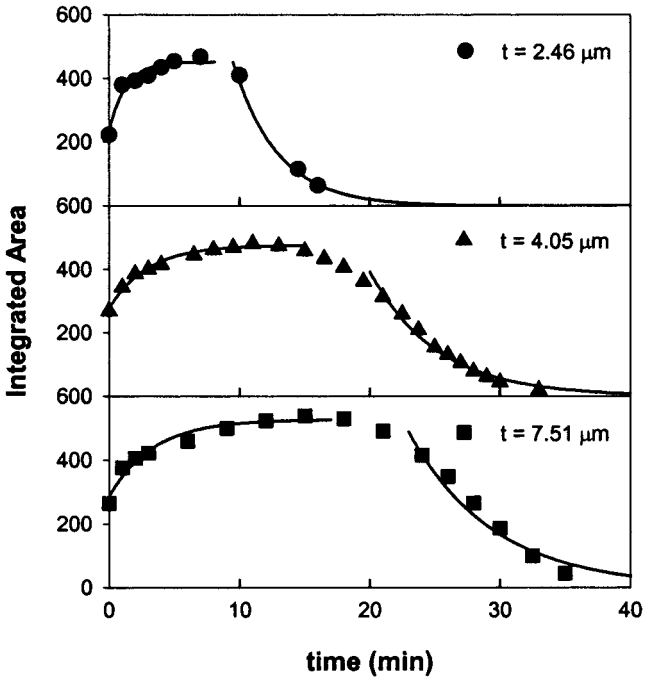

Figure 8. Evaporation of water of three different thickness PVDF films monitored by specular reflectance IR spectroscopy for films remaining on the silicon substrate. The area under the −OH region is plotted as a function of time. Two first-order rate constants were found for each film. Solid lines are the fits for first-order processes. Top: circles, $t = 2.46\ \mu$m, $k_1 = 0.81\ \text{min}^{-1}$, $k_2 = 0.29\ \text{min}^{-1}$. Middle: triangles, $t = 4.05\ \mu$m, $k_1 = 0.34\ \text{min}^{-1}$, $k_2 = 0.19\ \text{min}^{-1}$. Bottom: squares, $t = 7.51\ \mu$m, $k_1 = 0.30\ \text{min}^{-1}$, $k_2 = 0.15\ \text{min}^{-1}$.

ing the 20 min lag time. The time dependence of the integrated area was significantly more complicated for these cases, as shown in Figure 8. Again, the rate constants depend on the film thickness and the relative humidity. The change in water content in the film is puzzling. In all cases investigated thus far, there is an initial increase in the water content in the film followed by a much slower loss. The two time regions can be modeled independently using first-order kinetics with the rate constant for the fast process being roughly twice as large as the rate constant for the slow process. We attribute the initial rise in the water content, at least in part, to condensation of gas-phase water by a local cooling of the film surface by the rapid loss of the more volatile acetone.

The kinetics of water loss for films created from solutions with calcium nitrate tetrahydrate are even more complex. The water loss displays at least three different rate processes apparent in the data. Satisfactory extraction of rate constants has not been obtained yet, but further experiments are being pursued.

We have found no model that can explain the data. Since both the short time and long time rate constants depend on film thickness, at least two diffusion constants are required. The fast time process is likely associated with evaporation of solvent from a thin layer near the surface of the film. This may be associated with the different polymer relaxation constants found for surface and bulk polymers similar to that recently reported for polystyrene.[34] The humidity dependence implies that a choice of absorption isotherm is required, but it is likely that the usual assumption that a local equilibrium is quickly established at the surface is invalid.

The surface roughness of the films appears to be a consequence of the fast kinetic process. This is a qualitative conclusion based on two observations. The results found from changing the average velocity while spin coating showed higher surface roughness (white films) at higher average velocity where the solvent is forced out of the film more quickly. (Solvent evaporation rates are greater at faster rotational velocities.) We also observed white films from all of the reflectance IR kinetic measurements with larger rate constants for the fast process. Thus, it may be that reconstruction of the surface layer may be responsible for both the development of surface roughness and the fast kinetic response. Further investigations will be required to test this hypothesis.

Conclusion

We reported the influence of water on the crystalline phase and surface morphology of PVDF thin films. We found that PVDF crystallizes in the unoriented polar β phase when adding a hydrated salt to the polymer solution or by use of a hygroscopic solvent such as DMSO at elevated humidity to deposit the polymer film. However, simply adding water to a polymer solution did not induce the polar crystalline form presumably because of the evaporation of the water. Thus, the essential feature for depositing PVDF directly to the β-phase from solution is to force water to remain in the drying film for a sufficiently long period of time. It is likely that hydrogen bonding between the water and the polar C−F bonds is responsible for this phase control.

At least two different kinetic processes can be identified as the films dry. The fast process is thought to be associated with a thin surface layer where solvent exchange with the gas phase surroundings occurs. Although the thickness of this surface layer could not be measured, it is likely to be about the same as the surface roughness, a few tenths of a micrometer, depending upon the humidity conditions. The slow process also depends on film thickness and is assigned to processes in the bulk of the film. The rate constants for the slow process also depend on the gas-phase humidity. Further work is required to establish a quantitative model of the kinetic processes.

Acknowledgment. The URI Sensors and Surface Technology Partnership and the URI Foundation provided financial support for this research project. We also thank Muhammad Shloul for measuring some of the IR spectra and Dr. Dongsheng Bu for performing the principal component analysis calculation.

References and Notes

(1) Kepler, R. G.; Anderson, R. A. *J. Appl. Phys.* **1978**, *49*, 4490.
(2) Omote, K.; Ohigashi, H. *J. Appl. Phys.* **1997**, *81*, 2760.
(3) Zhao, Z. X.; Bharti, V.; Zhang, Q. M. *Appl. Phys. Lett.* **1998**, *73*, 2054.
(4) Furukawa, T. *IEEE Trans. Electr. Insul.* **1989**, *24*, 375.
(5) Chan, H. L.; Zhao, Z.; Kwok, K. W.; Choy, C. L. *J. Appl. Phys.* **1996**, *80*, 3982.
(6) McFee, J. H.; Bergman, J. G.; Crane, G. R. *Ferroelectrics* **1972**, *3*, 305.
(7) Gao, Q.; Scheinbeim, J. I. *Macromolecules* **2000**, *33*, 7564l.
(8) Davis, G. T.; McKinney, J. E.; Broadhurst, M. G.; Roth, S. C. *J. Appl. Phys.* **1978**, *49*, 4998.
(9) Prest, W. M.; Luca, D. J. *J. Appl. Phys.* **1978**, *49*, 1978.
(10) Hsu, J. C.; Geil, P. H. *J. Mater. Sci.* **1989**, *24*, 1219.
(11) Kim, B. S.; Lee, J. Y.; Porter, R. S. *Polym. Eng. Sci.* **1989,** *38*, 1359.

(12) Beaulieu, R. *J. Appl. Phys.* **1996**, *79*, 8038.
(13) Tashiro, K.; Itoh, Y.; Kobayashi, M.; Tadokoro, H. *Macromolecules* **1985**, *18*, 2600.
(14) Kaura, T.; Nath, R.; Perlman, M. M. *J. Phys. D* **1991**, *24*, 1848.
(15) Hsu, S. L.; Lu, F. J.; Waldman, D. A.; Muthukumar, M. *Macromolecules* **1985**, *18*, 2583.
(16) Miller, R.; Raisoni, J. *J. Polym. Sci.* **1976**, *14*, 2326.
(17) Tawansi, A.; Abdel-Razek, E. M.; Zidan, H. M. *J. Mater. Sci.* **1997**, *32*, 6243.
(18) Prest, W. M.; Luca, D. J. *J. Appl. Phys.* **1975**, *46*, 4136.
(19) Kobayashi, M.; Tashire, K. *Macromolecules* **1975**, *8*, 158.
(20) Gregorio, R.; Cestari, M. *J. Polym. Sci.* **1994**, *32*, 859.
(21) Okuda, K.; Yoshida, T.; Sugita, M.; Asahina, M. *Polym. Lett.* **1967**, *5*, 465.
(22) Osaki, S.; Ishida, Y. *J. Polym. Sci.* **1975**, *13*, 1071.
(23) Gregorio, R.; Souca Nocita, N. C. *J. Phys. D* **1995**, *28*, 432.
(24) Tashiro, K.; Kobayashi, M.; Tadokoro, H. *Macromolecules* **1981**, *14*, 1757.
(25) Tashiro, K.; Itoh, Y.; Kobayashi, M.; Tadokoro, H. *Macromolecules* **1985**, *18*, 2601.
(26) Dikshit, A. K.; Nandi, A. K. *Macromolecules* **2000**, *33*, 2616.
(27) Cortili, G.; Zerbi, G. *Spectrochim. Acta* **1967**, *23A*, 285.
(28) Takeshi, H.; Masashi, K.; Hiroji, O. *J. Appl. Phys.* **1996**, *79*, 2016.
(29) Benz, M.; Euler, W. B.; Gregory, O. J. *Langmuir* **2001**, *17*, 239.
(30) Lai, J. H. *Polym. Eng. Sci.* **1979,** *19*, 1117.
(31) Mueller-Buschbaum, P.; Gutmann, J. S.; Wolkenhauer, M.; Stamm, M.; Smiligies, B.; Petry, W. *Macromolecules* **2001**, *34*, 1369.
(32) Jandt, K. D.; Heier, J.; Bates, F. S.; Kramer, E. J. *Langmuir* **1996**, *12*, 3716.
(33) Washo, B. D. *IBM J. Res. Dev.* **1977**, *14*, 190.
(34) Wallace, W. E.; Fischer, D. A.; Efimenko, K.; Wu, W. L.; Genzer, J. *Macromolecules* **2001**, *34*, 5081.

MA011744F